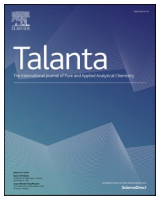
Talanta 266 (2024) 125066



Contents lists available at ScienceDirect

Talanta

journal homepage: www.elsevier.com/locate/talanta





High-sensitive and rapid electrochemical detection of miRNA-31 in saliva using Cas12a-based 3D nano-harvester with improved *trans*-cleavage efficiency

Yu Wu [1], Jingwen Pei [1], Yi Li, Guobin Wang, Lan Li, Jinbo Liu [**], Gang Tian [*]

Department of Laboratory Medicine, The Affiliated Hospital of Southwest Medical University, Luzhou, Sichuan, 646000, China

ARTICLE INFO

Handling Editor: Manel del Valle

Keywords:
MiRNA testing
CRISPR/Cas12a
Nanomachine
Electrochemical biosensor

ABSTRACT

Salivary miRNA-31 is a reliable diagnostic marker for early-stage oral squamous cell carcinoma (OSCC), but accurate detection of miRNA-31 in saliva samples is a challenge because of its low level and high sequence homology. The CRISPR/Cas12a system has the exceptional potential to enable simple nucleic acid analysis but suffers from low speed and sensitivity. To achieve rapid and high-sensitive detection of miRNA-31 using the CRISPR/Cas12a system, a Cas12a-based nano-harvester activated by a polymerase-driven DNA walker, named as dual 3D nanorobots, was developed. The target walked rapidly on the surface of DNA hairpin-modified magnetic nanoparticles driven by DNA polymerase, generating numerous double-strand DNA (dsDNA). Then, the Cas12a bound to the generated dsDNA for activating its *trans*-cleavage activity, forming 3D nano-harvester. Subsequently, the harvester cut and released methylene blue-labeled DNA hairpins immobilized on the sensing interface, leading to the change in electrochemical signal. We found that the *trans*-cleavage activity of the harvester was higher than the conventional CRISPR/Cas12a system. The developed dual 3D nanorobots could enable rapid (detection time within 60 min), high-sensitive (detection limit of femtomolar), and specific analysis of miRNA-31 in saliva samples. Thus, our established electrochemical biosensing strategy has great potential for early diagnosis of OSCC.

1. Introduction

Oral squamous cell carcinoma (OSCC) is one of the highly prevalent malignancies worldwide [1], which is usually diagnosed late because of the few and inconspicuous clinical features in the early stage. The five-year survival rate of patients with advanced OSCC is only 20% [2]. Despite the current advances in treatment, the improvement in the survival rate of oral squamous cell carcinoma patients is minimal [3,4]. Therefore, the development of strategies for early diagnosis of OSCC is of great importance. Liquid biopsy has shown great clinical value in multi-omic analysis of cancer. Compared to blood (serum and plasma), saliva is an ideal sample for non-invasive biomarker detection [5,6]. It has been shown that miRNA-31 in the saliva is a sensitive tumor marker for early diagnosis of OSCC [7]. However, accurate analysis of miRNA-31 in saliva samples is a challenge owing to its low number, short sequence (21 nt), and high sequence homology.

Traditional methods for miRNAs detection, including northern blotting and quantitative reverse transcription polymerase chain reaction (qRT-PCR), expose time-consuming, cumbersome primer design, and the need for expensive instruments and professionally trained medical testers [8,9]. Accordingly, many researchers have started to try to develop new strategies for miRNAs detection [10,11]. Among them, electrochemical biosensing platforms based on DNA nanomachines show great promise in exploring efficient signal amplification and highly sensitive detection strategies for miRNAs [12–14]. DNA walker is one of the DNA nanomachines, which allows to accomplish amplified signal output due to the fact that the walking strands continuously move along walking tracks under the action of driving forces [15,16]. Compared with strand displacement reactions-based DNA walkers, protein enzymatic reactions (endonuclease and exonuclease) based-DNA walkers have higher walking efficiency [17,18]. Among enzyme-involved isothermal amplification reactions, “invading stacking primer”

* Corresponding author.
** Corresponding author.
E-mail addresses: liujb7203@swmu.edu.cn (J. Liu), tiangang@swmu.edu.cn (G. Tian).
[1] These authors contributed equally to this work.

https://doi.org/10.1016/j.talanta.2023.125066
Received 10 March 2023; Received in revised form 11 May 2023; Accepted 7 August 2023
Available online 10 August 2023
0039-9140/© 2023 Published by Elsevier B.V.

amplification reaction (ISAR) reveals high reaction rate, high sensitivity, and superior selectivity for the detection of miRNAs [19,20]. The ISAR technology is based on target-induced change in the hybridization position of primers and the primer-invaded toehold exchange and stack hybridization reactions [21]. However, ISAR-based DNA walker has been unexplored.

Acting as attractive diagnostic technologies, clustered regularly interspaced short palindromic repeats (CRISPR) systems and CRISPR-associated (Cas) enzymes, such as Cas12a and Cas13a, have presented great advantages [22]. Particularly, the *trans*-cleavage activity of Cas12a can be activated by the specific recognition of double-strand DNA (dsDNA) or single-strand DNA (ssDNA) with a complementary guide RNA (gRNA), which triggers cleavage and release of reporter molecules [23,24]. The cas12a-based methods have been applied to the sensing of various targets including pathogens, proteins, small molecules, and so on [25–27], but long reaction times limit their detection sensitivity and speed. To this end, various strategies have been used to enhance the *trans*-cleavage efficiency of Cas12a, such as replacing linear ssDNA reporters with hairpin DNA probes or Au-nanobeacon (DNA hairpin-modified Au nanoparticles) due to the improved affinity of Cas12a to hairpin structures [28,29], using chemical enhancers for acting on the hybridization of gRNA and target nucleic acids [30], engineering crRNA by extending its 3′- or 5′-ends with DNA [31], and designing multiplex crRNA to hybridize different regions of the same dsDNA target [32]. Nevertheless, these strategies may require high testing costs because of the use of fluorophore/quencher pair, extra chemical reagents, chimeric DNA/RNA guide, or multiplex crRNA. Therefore, new strategies for increasing the speed and sensitivity of Cas12-based sensing methods are needed.

Responding to the above considerations, we developed a dual 3D nanorobot, the combination of ISAR-based DNA walker and Cas12a-based nano-harvester, for high-sensitive and rapid detection of salivary miRNA-31. The target miRNA is captured by DNA hairpin-modified magnetic nanoparticles (DH-MNs) and undergoes a walking process (ISAR-based walker) to form multiple DNA duplexes which are then combined with crRNA-Cas12a, assembling the 3D nano-harvester to cut and release the methylene blue-labeled hairpin probes (MB-HP) from the sensing interface, thus resulting in a significant signal change. The Cas12a-based nano-harvester possesses enhanced *trans*-cleavage efficiency. Detecting miRNA-31 in saliva samples shows that this developed biosensor is a fast, high-sensitive, and highly selective sensing platform and has good potential for early diagnosis of OSCC.

2. Experimental section

2.1. Materials and reagents

HPLC-purified DNA, RNA, crRNA sequences (Table S1), tris(2-carboxyethy) phosphine hydrochloride (TCEP), diethyl pyrocarbonate (DEPC), deoxynucleotide triphosphates (dNTP), and 4S Red Plus Nucleic Acid Stain were obtained from Sangon Biotech Co, Ltd. (Shanghai, China). Polyethylene glycol sorbitan monolaurate (Tween-20) was purchased from Sigma-Aldrich (St. Louis, USA). Phosphate buffered saline (PBS) buffer (RNAase and DNAase free, 0.01 M, pH = 7.2–7.5) was purchased from SenBeiJia Biological Technology Co, Ltd (China, Nanjing). Bst 2.0 polymerase, EnGenLba Cas12a, and NEB buffer2.1 were purchased from New England Biolabs (Ipswich, MA, U.K.). Streptavidin magnetic nanoparticles (MNs) were purchased from Beyotime (Shanghai, China). All chemical reagents were of analytical grade, and all solutions were treated with 1% DEPC to prevent the effect of ribonuclease.

2.2. Apparatus and measurements

All electrochemical experiments were performed on a CHI660D electrochemical workstation (Shanghai Chenhua Instruments Co, Ltd, China) with a three-electrode system consisting of a gold electrode (working electrode), a platinum wire electrode (counter electrode) and an Ag/AgCl electrode (reference electrode). Malvern Particle Size Analyzer (ZATA potential distribution, UK) was applied to characterize the potentials of nanomaterials. Polyacrylamide gel images were characterized with GelDoc XR + System (Bio-Rad, USA).

2.3. Preparation of DH-MNs

First, 20–100 μl of well-mixed MNs were placed in a centrifuge tube and separated on a magnetic stand for 1 min to remove the supernatant. Then add TBS solution and wash for 30 s, magnetic separation to remove the supernatant, repeat three times, and finally wash with 0.05 M and 0.1 M NaCl (DEPC water treatment) respectively for the last time. Resuspend the MNs with 2 times the volume of binging/washing buffer (2X), then add excess biotin-labeled DNA hairpins and mix well, incubate for 10 min at room temperature to saturate the MNs, and verify the successful binding of biotin-labeled DNA hairpins on the MNs with UV spectrophotometer. Subsequently, wash the beads repeatedly with binging/washing buffer (1X) 2–3 times, and remove the supernatant. Finally, the synthesized DH-MNs were resuspended and stored at 4 °C for use.

2.4. Preparation of the biosensing electrode

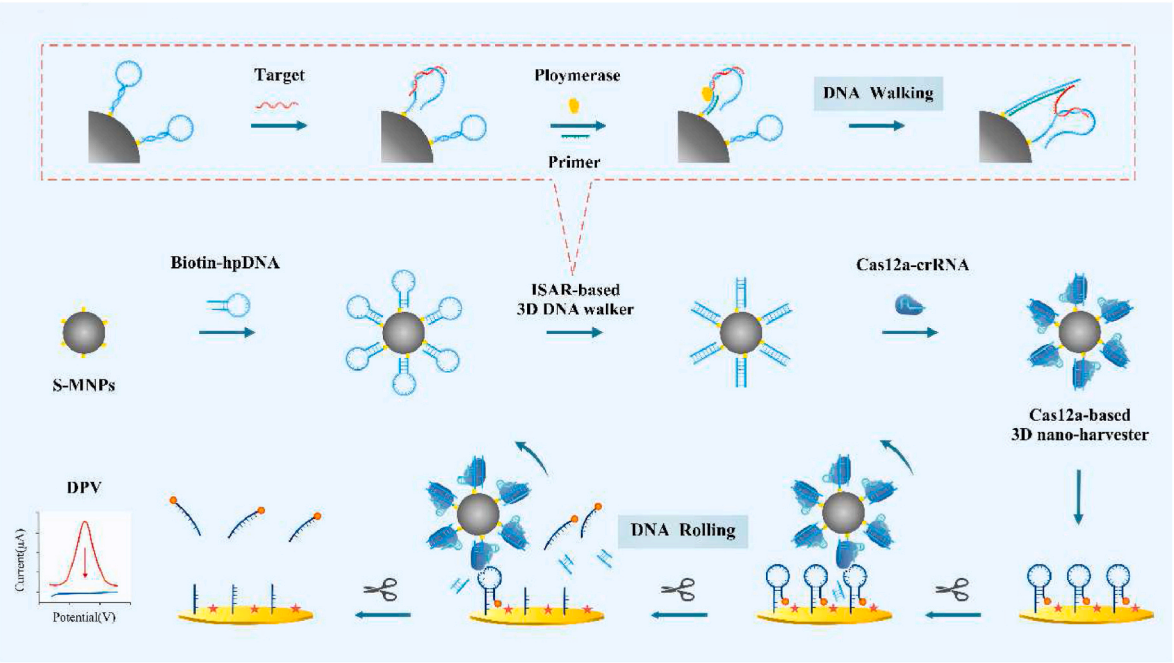
Polishing the gold electrode with 0.3 μm and 0.05 μm alumina powder respectively for 5 min until the electrode surface is smooth as a mirror, then put it into anhydrous ethanol and deionized water in turn (the electrode surface should not touch the beaker wall) for ultrasonic cleaning, and blow dry with N_2 gas. After that, the electrode was immersed in piranha solution ($H_2SO_4/H_2O_2 = 3:1$) for 15 min to remove organic impurities from the electrode surface, and rinsed with water at the end. Incubate the MB-HP before placing the electrode in 0.5 M H_2SO_4 for CV scanning. The MB-HP was dissolved in 100 mM Tris-HCl buffer solution (containing 10 mM TCEP, 5 mM $MgCl_2$, 0.5 M NaCl, pH 7.4). Then 10 μL of 1 μm MB-HP was added dropwise to the gold electrode surface and incubated at 4 °C for 12 h. After the formation of the methylene blue sequence monolayer, the modified electrode was treated with 1 mM 6-Mercapto-1-hexanol (MCH) to close the unbound and empty spaces to reduce non-specific adsorption. Finally, wash thoroughly with washing buffer (10 mM PBS containing 0.05% (w/v) Tween-20, pH 7.4).

2.5. Detection of miRNA-31 using the developed dual 3D DNA nanorobots

To operate the ISAR-based 3D DNA walker, 10 μL of target with different concentrations was added to 10 μL of Solution A (varying amounts of primer and polymerase, 1 mM dNTP, and 2 μL of the DH-MNs) and incubated for 30 min at 37 °C. Then, 10 μL of Solution B (45 nM crRNA, 50 nM Cas12a, 10 U RNase inhibitor, and 1 × NEB buffer) was added to the above-mentioned mixture and incubated for 5 min at 37 °C. Finally, 10 μL of the mixed solution was added dropwise to the modified gold electrode and incubated for 30 min at 37 °C for triggering the Cas12a-based 3D nano-harvester. The treated electrode was washed for DPV testing, and the test solution was PBS. The DPV parameters: Init E −0.5 V, Final E 0 V, Incr E 0.004 V, Amplitude 0.05 V. EIS tests were performed with 5 mM Fe $(CN)_6^{3-/4-}$ as the electrolyte. The parameters of EIS: biasing potential 0.204 V, amplitude 5 V, frequency range 0.1 Hz–100 kHz.

2.6. Polyacrylamide gel electrophoresis (PAGE) electrophoresis

Preparation of 12% polyacrylamide gels to validate the process of



Scheme 1. Electrochemical biosensor principle of Cas12a-based 3D nano-harvester activated by ISAR-based 3D DNA walker for salivary miRNA-31 detection.

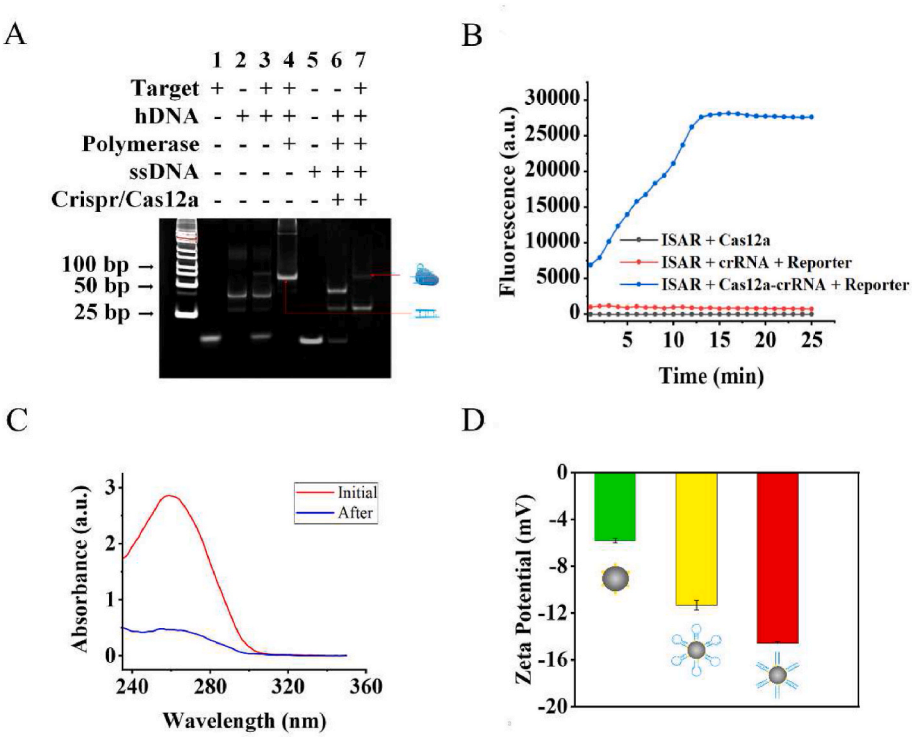


Fig. 1. Feasibility study of the dual 3D nanorobots based on the ISAR-based walker and Cas12-based nano-harvester. (A) PAGE of the ISAR and Cas12a reaction, the final concentration of ssDNA added to lanes 6 and 7 was equal. (B) Verification of the activation of the dsDNA ISAR produced to the *trans*-cleavage activity of Cas12 by fluorescence experiments. (C) Verification of the binding of hpDNA to MNs by UV–vis absorption spectrophotometer. (D) Variation of the ζ-potential of the bare MNs, the DH-MNs, and the dsDNA-tethered MNs. The dsDNA was produced by the ISAR reaction. Error bars are standard deviation obtained from three independent experiments.

ISAR and the activity of Cas12a. Electrophoresis was performed in 0.5 × TBE buffer (80 mM Tris-boric acid, pH 8.3) at a 120 V constant voltage for 60 min before staining with SYBR II nucleic acid dye.

3. Results and discussion

3.1. Design principles of the dual 3D nanorobots

The working principle of the biosensor was described in Scheme 1. In the presence of target miRNA, the DNA hairpin of the DH-MNs was opened by hybridizing with the target. Then the designed primer bound to the opened hairpin and was gradually extended to displace the target with the cooperation of DNA polymerase, meanwhile forming a dsDNA. Subsequently, the displaced miRNA continued to participate in the next reaction. In this way, the target could constantly move on the surface of MNs, which transformed a large amount of dsDNA. The ISAR-based 3D DNA walker was more convenient and faster for the constant temperature cycling reaction, avoiding traditional thermal cycler. As the

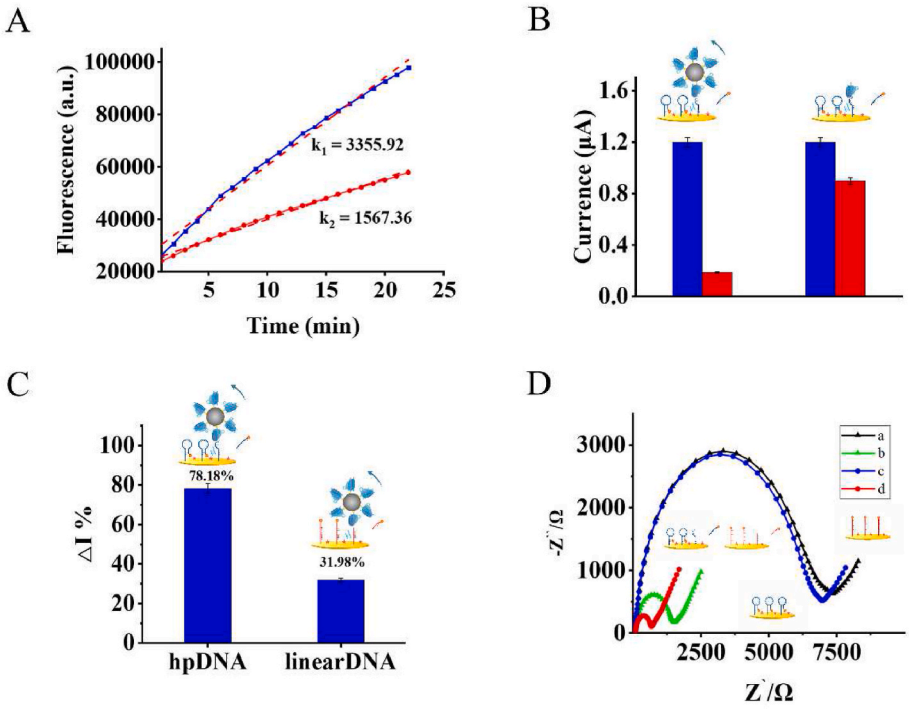


Fig. 2. Verification of the high tris-cleavage efficiency of the Cas12a-based nano-harvester. (A) Comparison of fluorescence experiments results of the cleavage efficiency of the Cas12a-based 3D nano-harvester and the conventional Cas12a system for FQ-ssDNA. (B) Comparison of DPV signals of the cleavage efficiency of Cas12a-based 3D nano-harvester and the conventional Cas12a system for MB-HP. (C) Compare the different effects of the nano-harvester shearing MB-ssDNA and MB-HP reporters separately. (D) EIS of the MB-ssDNA and MB-HP modified on gold electrodes before and after the onset of the shearing process respectively. Error bars are standard deviation obtained from three independent experiments.

amplification product of ISAR, dsDNA could be recognized by the designed crRNA. The crRNA that included a repetitive sequence and an editable target recognition sequence, bound to Cas12a to form a crRNA-Cas12a duplex. The duplex specifically recognized the dsDNA based on the crRNA's recognition sequence and the protospacer adjacent motif (PAM) of the dsDNA, which activated the *cis*-cleavage and *trans*-cleavage activity of Cas12a to form the nano-harvester. Subsequently, the Cas12a-based nano-harvester cleaved the loop structure of the MB-HP and then released the reporter probes, thus producing a significant DPV signal change.

3.2. Mechanism study of the ISAR-activated Cas12a method

To verify that the ISAR and Cas12a could react successfully, we took PAGE to validate the ability of ISAR to generate dsDNA and the ability of Cas12a to cleave non-specific ssDNA. As shown in Fig. 1A, compared to hairpin DNA (hpDNA) in lane 2, the target and hairpin DNA (hpDNA) could not effectively form dsDNA (lane 3). The ISAR could only occur when the target, hpDNA, primer, and polymerase were involved simultaneously (lane 4). In the absence of target, the dsDNA could not be generated and the ssDNA could not be sheared (lane 6). In contrast, in the presence of the target, the crRNA-Cas12a was activated by the ISAR-produced dsDNA and sheared the ssDNA (lane 7). In addition, real-time fluorescence experiments were also used for evaluating the ISAR-activated Cas12a method (Fig. 1B). In the absence of target, Cas12a, or 5′-FAM and 3′-BHQ-labeled ssDNA (FQ-ssDNA), these systems produced ignorable fluorescence signals. However, when the target was added to the whole system, a rapidly rising fluorescence signal was observed, implying that the ISAR-produced dsDNA activated the *trans*-cleavage activity of Cas12a for cleaving FQ-ssDNA, leading to the recovery of FAM fluorescence. These results demonstrated that the cascade amplification reaction based on the ISAR and Cas12a was feasible.

3.3. Characterization of the ISAR-based 3D DNA walker

We firstly evaluated the binding of the biotin-labeled hpDNA to the pre-washed MNs by UV–Vis absorption spectra. As shown in Fig. 1C, compared to the initial hpDNA solution, the absorption value at 260 nm of the suspension via magnetic separation was greatly reduced, indicating that the hpDNA was successfully bound to the MNs. Next, to demonstrate whether the target could move on the surface of MNs, we performed ζ-potential analysis. As shown in Fig. 1D, the MNs themselves were negatively charged. After the MNs were modified with hpDNA, the ζ-potential of the DH-MNs became more negative because the nucleic acid nature of the DNAs was negatively charged. With the addition of targets, a further decrease in the ζ-potential of the end-products was observed, indicating that numerous dsDNA was produced on the MNs (dsDNA-tethered MNs), which was because the target could move on the surface of MNs powered by DNA polymerase. These results suggested that the ISAR-based 3D DNA walker was successfully developed.

3.4. High tris-cleavage efficiency of the Cas12a-based nano-harvester

To highlight the high tris-cleavage efficiency of the Cas12a-based nano-harvester, the conventional Cas12a system was compared under identical conditions. We calculated that the combining quantity of the synthesized dsDNA by ISAR to the MNs was about 142 μg/μL (Fig. S1), and the same concentration of dsDNA was also added to the conventional Cas12a system. In the liquid phase environment, the Cas12a-based nano-harvester exhibited higher *trans*-cleavage efficiency and released more fluorescence with a linear slope (K1) = 3355.92, while the conventional Cas12a system exhibited relatively low cleavage efficiency with a linear slope (K2) = 1567.36 (Fig. 2A). Then, the two systems were applied to gold electrodes modified with the MB-HP probes to evaluate their cleavage efficiency at the solid-liquid interface. As shown in Fig. 2B, the change in DPV signal of the nano-harvester was bigger than that of the conventional Cas12a system, implying that the cleavage ability of the nano-harvester was much greater than that of the conventional Cas12a system. These results demonstrated that the nano-harvester possessed higher cutting efficiency in both homogeneous and heterogeneous conditions.

To investigate the cleavage ability of the nano-harvester on the gold electrode for different reporter probes, we compared the different DPV responses of the nano-harvester to the MB-HP [33] and linear MB-labeled ssDNA (MB-ssDNA) under the same experimental

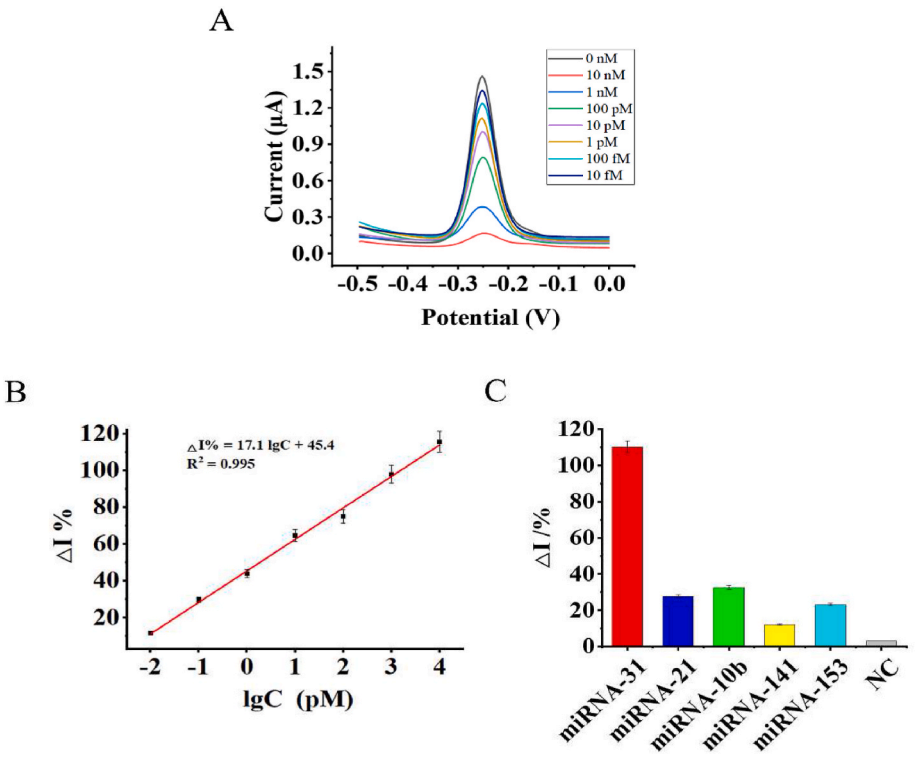


Fig. 3. Evaluation of the analysis performance of the developed biosensor. (A) Typical DPV curves responding to 0, 10 nM, 1 nM, 100 pM, 10 pM, 1 pM, 100 fM, and 10 fM target miRNA-31. (B) The calibration curve for the ΔI% versus the logarithm of target miRNA. (C) Investigation of the specificity of the biosensor by comparing DPV signals responding to different miRNAs. Error bars are standard deviation obtained from three independent experiments.

conditions, respectively. As shown in Fig. 2C, the peak current of the linear MB-ssDNA decreased from 1.14 μA to 0.78 μA, producing a nearly 31.98% change in current. Then when the gold electrode was incubated with the MB-HP, the initial background peak current was significantly higher (1.41 μA). The reason for the higher initial current of the MB-HP is that the MB can approach the gold electrode surface more easily, so it is more favorable for electron transfer [34]. After performing the cut, the peak current dropped substantially to 0.307 μA. The current change of the MB-hpDNA probe was approximately 78.18%. Therefore, the Cas12a-based nano-harvester exhibited higher cleavage efficiency for MB-hpDNA.

Furthermore, the higher cleavage efficiency of the nano-harvester for MB-hpDNA was evaluated by EIS. Fig. 2D respectively shows the EIS of the gold electrodes modified with the MB-ssDNA and the MB-HP, in 5 mM $[Fe(CN)_6]^{3-/4-}$ solution, before and after being cut by the nano-harvester. The MB-ssDNA-modified electrode showed slightly higher resistance than the MB-HP-modified electrode before cleavage occurred, indicating a higher density of MB-ssDNA on the gold electrode under incubation with two identical concentrations of probes. However, after cleavage occurred, the MB-HP-modified electrode showed a smaller resistance, indicating that the nano-harvester exhibited greater cleavage efficiency for the MB-HP modified on the gold electrode surface. These results demonstrate that the use of MB-HP-modified gold electrodes is more effective in reducing the spatial site resistance effect, allowing the nano-harvester to cut DNA more efficiently.

3.5. Optimization of detection conditions

To obtain the best sensing performance, we optimized some key parameters in our experiments, which were applied in the subsequent experiments. We chose to use 1 μM MB-HP to incubate the gold electrode to obtain a stable and high-quality background signal. First, we discussed the optimal time and temperature for the formation of ISAR products that could activate the nano-harvester by measuring fluorescence intensity. As shown in Fig. S2A, the reaction of the ISAR-based DNA walker at 37 °C for 30 min could maximally activate the cleavage ability of the nano-harvester. Then, the effect of DNA polymerase concentration from 4 U to 12 U on the DPV signal was examined separately. In Fig. S2B, DNA polymerase concentration at 8 U produced a greater change in DPV peak current (ΔI), and a plateau was reached after 8U, so we chose to use 8 U DNA polymerase for the ISAR reaction. In addition, the *trans*-cleavage was strongly influenced by time on the gold electrode surface. As shown in Fig. S2C, with increasing *trans*-cleavage time, ΔI also gradually increased and reached a maximum at 30 min, indicating that the inverse cutting was time-dependent. Afterward, there was a slight decrease in ΔI, probably because the reaction solution on the electrode surface had evaporated to some extent, which prevented the nano-harvester from moving sufficiently on the electrode surface.

3.6. Sensor performance analysis

After determining the optimal experimental conditions, we set a series of miRNA-31 concentrations to examine the biosensor sensitivity. Fig. 3A shows that the DPV electrochemical signal becomes smaller as the target concentration increases from 10 fM to 10 nM. The current change of DPV (ΔI) correlated well with the logarithm of miRNA-31 concentration in the range of 10 fM to 10 nM. The regression equation was ΔI% = 17.1 lgC+ 45.4 (R^2 = 0.995), and the limit of detection (LOD) was 3.5 fM (3σb/slope) (Fig. 3B). Compared with other electrochemical biosensors for miRNAs detection, as shown in Table S2, the developed biosensor has an excellent performance in terms of time, linear range, and LOD. In addition, we tested several miRNAs similar to the target by comparing the response signals they produced and determining whether there was cross-reactivity at the same concentration (10 nM). These miRNAs included miRNA-31 as the positive experimental group, miRNA (NC) as the negative control group, as well as miRNA-141, miRNA-153, miRNA-21, and miRNA-10b as non-specific

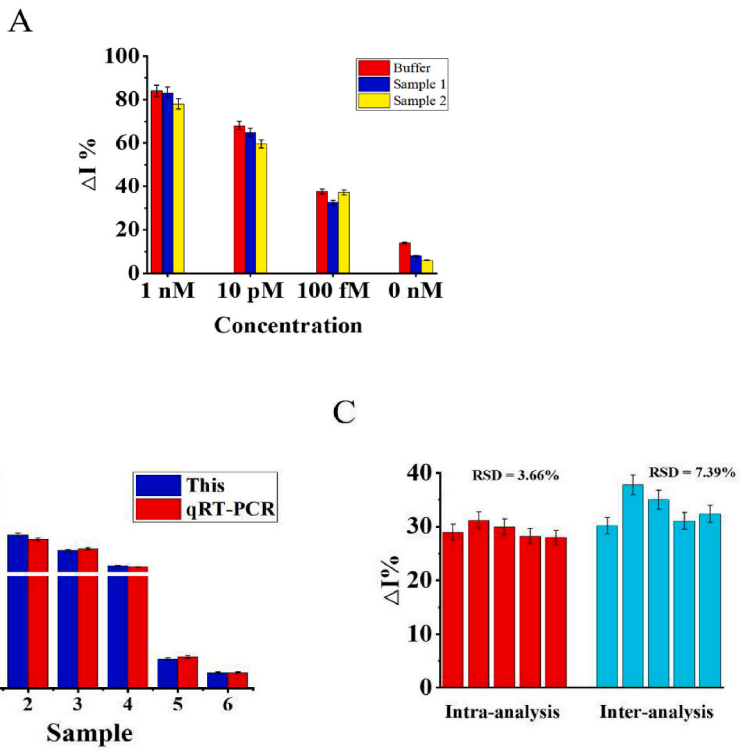


Fig. 4. (A) Evaluation of the detection ability of the biosensor in real samples by testing 1 nM, 10 pM, 100 fM, 0 nM target miRNA in buffer and saliva. (B) Methodological comparison of the proposed biosensor with qRT-PCR. 1–4 are samples from patients with oral squamous cell carcinoma, 5 and 6 are samples from healthy individuals. (C) Evaluation of the reproducibility of the biosensor by detecting 100 fM target. Error bars are standard deviation obtained from three independent experiments.

miRNAs. As can be seen in Fig. 3C, the constructed biosensor has high selectivity for target miRNA-31, which is attributed to the high recognition of target miRNAs by the specially designed hpDNA. Also, the specific recognition of duplex by downstream Cas12a-based nano-harvester provides a further guarantee for the high specificity of the whole strategy.

3.7. Detection of miRNA-31 in real saliva samples

To determine whether the developed biosensor could be applied to the detection of miRNAs in real clinical samples, we added a certain amount of miRNA-31 to two healthy human saliva that had been centrifuged and diluted. The final concentrations of miRNA-31 in saliva samples were 1 nM, 10 pM, and 100 fM, respectively. Fig. 4A shows that the sensor can sensitively detect target miRNAs with a small degree of influence by the biological environment, both in standard buffers and in complex real samples. We measured the specific percent recovery of 93.9%–107.8% in five samples of 10 pM target concentration. To verify whether the biosensor can be applied to the detection of miRNA-31 in the saliva of real oral squamous cell cancer patients, we tested saliva samples from four patients and two healthy individuals. The results are shown in Fig. 4B, where the four patients produced significantly higher signals than healthy individuals. And there was good agreement by comparison with qRT-PCR analysis, which proved the reliability of the developed electrochemical biosensor. In addition, to verify the reproducibility of the biosensor, we performed five standard replicate experiments on 100 fM of target miRNA. The relative standard deviation (RSD) values of intra- and inter-assays are as low as 3.66% and 7.39%, indicating that the biosensor has good reproducibility (Fig. 4C).

4. Conclusion

In summary, we successfully developed a novel electrochemical biosensor based on the ISAR-based 3D DNA walker and the Cas12-based nano-harvester for high-sensitive and specific detection of salivary miRNA-31. Compared to conventional CRISPR/Cas12a system, the Cas12-based nano-harvester has higher *trans*-cleavage efficiency, which provides new horizons for enhancing *trans*-cleavage activity of Cas12a. The dual 3D nanorobots ensure considerable signal amplification efficiency, which makes the whole detection platform possess excellent sensitivity and specificity. The biosensor is able to achieve rapid, high-sensitive, and specific detection of miRNA-31 in saliva samples, showing great potential for early diagnosis of OSCC.

Credit author statement

Yu Wu: Conceptualization, Methodology, Software, Investigation, Writing - original draft. JingWen Pei: Conceptualization, Software, Investigation, Data curation. Yi Li: Software, Investigation. GuoBing Wang: Methodology, Formal analysis, Software. Lan Li: Software, Investigation. Jinbo Liu: Methodology, Funding acquisition, Resources, Validation. Gang Tian: Supervision, Methodology, Data curation, Funding acquisition, Project administration.

Declaration of competing interest

We declare that we have no financial and personal relationships with other people or organizations that can inappropriately influence our work, there is no professional or other personal interest of any nature or kind in any product, service and/or company that could be construed as influencing the position presented in, or the review of, the manuscript entitled "**Ultrasensitive and rapid electrochemical detection of miRNA-31 in saliva using Cas12a-based 3D nano-harvester with improved *trans*-cleavage efficiency**".

Data availability

Data will be made available on request.

Acknowledgment

This study was supported by grants from the Luzhou Science and

Technology Department Applied Basic Research program (No: 2022-JYJ-145), and the Sichuan Province Science and Technology Department of foreign (border) high-end talent introduction project (No: 2023JDGD0037), and the Luzhou City - School Industry-University Research Cooperation Cultivation Project (NO: 2020LZXNYD02), and the Sichuan Province Medical Association Youth Innovation Project (NO: Q22027).

Appendix A. Supplementary data

Supplementary data to this article can be found online at https://doi.org/10.1016/j.talanta.2023.125066.

References

[1] L.H. Bajrai, S.S. Sohrab, M. Mobashir, M.A. Kamal, M.A. Rizvi, E.I. Azhar, Understanding the role of potential pathways and its components including hypoxia and immune system in case of oral cancer, Sci. Rep. 11 (1) (2021), 19576, https://doi.org/10.1038/s41598-021-98031-7.

[2] M.J. Jeng, M. Sharma, T.Y. Chao, Y.C. Li, S.F. Huang, L.B. Chang, L. Chow, Multiclass classification of autofluorescence images of oral cavity lesions based on quantitative analysis, PLoS One 15 (2) (2020), e0228132, https://doi.org/10.1371/journal.pone.0228132.

[3] C.F. Poh, S.P. Ng, P.M. Williams, L. Zhang, D.M. Laronde, P. Lane, C. Macaulay, M. P. Rosin, Direct fluorescence visualization of clinically occult high-risk oral premalignant disease using a simple hand-held device, Head Neck 29 (1) (2007) 71–76, https://doi.org/10.1002/hed.20468.

[4] J. Young, M. Yee, H. Kim, J. Cheung, T. Chino, N. Düzgüneş, K. Konopka, Phototoxicity of liposomal Zn- and Al-phthalocyanine against cervical and oral squamous cell carcinoma cells in vitro, Med. Sci. Monit. 22 (2016) 156–164, https://doi.org/10.12659/msmbr.901039.

[5] J.W. Chen, J.H. Wu, W.F. Chiang, Y.L. Chen, W.S. Wu, L.W. Wu, Taxonomic and functional dysregulation in salivary microbiomes during oral carcinogenesis, Front. Cell. 11 (2021), 663068, https://doi.org/10.3389/fcimb.2021.663068.

[6] Y. Cui, H.S. Kim, E.S. Cho, D. Han, J.A. Park, J.Y. Park, W. Nam, H.J. Kim, I.H. Cha, Y.H. Cha, Longitudinal detection of somatic mutations in saliva and plasma for the surveillance of oral squamous cell carcinomas, PLoS One 16 (9) (2021), e0256979, https://doi.org/10.1371/journal.pone.0256979.

[7] L.L. Wang, H.X. Li, Y.Y. Yang, Y.L. Su, J.S. Lian, T. Li, J. Xu, X.N. Wang, N. Jin, X. F. Liu, MiR-31 is a potential biomarker for diagnosis of head and neck squamous cell carcinoma, Int. J. Clin. Exp. Pathol. 11 (9) (2018) 4339–4345.

[8] K.A. Cissell, S.K. Deo, Trends in microRNA detection, Anal. Bioanal. Chem. 394 (4) (2009) 1109–1116, https://doi.org/10.1007/s00216-009-2744-6.

[9] K. Yin, V. Pandian, K. Kadimisetty, X. Zhang, C. Ruiz, K. Cooper, C. Liu, Real-time colorimetric quantitative molecular detection of infectious diseases on smartphone-based diagnostic platform, Sci. Rep. 10 (1) (2020), https://doi.org/10.1038/s41598-020-65899-w, 9009.

[10] Y. Gao, H. Yu, J. Tian, B. Xiao, Nonenzymatic DNA-based fluorescence biosensor combining carbon dots and graphene oxide with target-induced DNA strand displacement for microRNA detection, Nanomaterials 11 (10) (2021) 2608, https://doi.org/10.3390/nano11102608.

[11] S. Jampasa, W. Wonsawat, N. Rodthongkum, W. Siangproh, P. Yanatatsaneejit, T. Vilaivan, O. Chailapakul, Electrochemical detection of human papillomavirus DNA type 16 using a pyrrolidinyl peptide nucleic acid probe immobilized on screen-printed carbon electrodes, Biosens. Bioelectron. 54 (2014) 428–434, https://doi.org/10.1016/j.bios.2013.11.023.

[12] D. Li, Y. Xu, L. Fan, B. Shen, X. Ding, R. Yuan, X. Li, W. Chen, Target-driven rolling walker based electrochemical biosensor for ultrasensitive detection of circulating tumor DNA using doxorubicin@tetrahedron-Au tags, Biosens. Bioelectron. 148 (2020), 111826, https://doi.org/10.1016/j.bios.2019.111826.

[13] P. Miao, Y. Tang, DNA walking and rolling nanomachine for electrochemical detection of miRNA, Small 16 (47) (2020), e2004518, https://doi.org/10.1002/smll.202004518.

[14] N. Wu, K. Wang, Y.T. Wang, M.L. Chen, X.W. Chen, T. Yang, J.H. Wang, Three-dimensional DNA nanomachine biosensor by integrating DNA walker and rolling machine cascade amplification for ultrasensitive detection of cancer-related gene, Anal. Chem. 92 (16) (2020) 11111–11118, https://doi.org/10.1021/acs.analchem.0c01074.

[15] L. Wang, Z. Meng, F. Martina, H. Shao, F. Shao, Fabrication of circular assemblies with DNA tetrahedrons: from static structures to a dynamic rotary motor, Nucleic Acids Res. 45 (21) (2017) 12090–12099, https://doi.org/10.1093/nar/gkx1045.

[16] J. Li, W. Wang, H. Zhang, Z. Lu, W. Wu, M. Shu, H. Han, Programmable DNA tweezer-actuated SERS probe for the sensitive detection of AFB (1), Anal. Chem. 92 (7) (2020) 4900–4907, https://doi.org/10.1021/acs.analchem.9b04822.

[17] K. Yehl, A. Mugler, S. Vivek, Y. Liu, Y. Zhang, M. Fan, E.R. Weeks, K. Salaita, High-speed DNA-based rolling motors powered by RNase H, Nat. Nanotechnol. 11 (2) (2016) 184–190, https://doi.org/10.1038/nnano.2015.259.

[18] L. Song, Y. Zhuge, X. Zuo, M. Li, F. Wang, DNA walkers for biosensing development, Adv. Sci. 9 (18) (2022), e2200327, https://doi.org/10.1002/advs.202200327.

[19] W. Liu, M. Zhu, H. Liu, J. Wei, X. Zhou, D. Xing, Invading stacking primer: a trigger for high-efficiency isothermal amplification reaction with superior selectivity for detecting microRNA variants, Biosens. Bioelectron. 81 (2016) 309–316, https://doi.org/10.1016/j.bios.2016.02.073.

[20] M. Wang, Y. Zhou, H. Yin, W. Jiang, H. Wang, S. Ai, Signal-on electrochemiluminescence biosensor for microRNA-319a detection based on two-stage isothermal strand-displacement polymerase reaction, Biosens. Bioelectron. 107 (2018) 34–39, https://doi.org/10.1016/j.bios.2018.02.015.

[21] M. Chen, H. Li, Z. Shi, W. Peng, Y. Qin, R. Luo, D. Zhou, X. Gong, J. Chang, High fluorescence quenching probe-based reverse fluorescence enhancement LFTS coupling with IS-primer amplification reaction for the rapid and sensitive Parkinson Disease-associated MicroRNA detection, Biosens. Bioelectron. 165 (2020), 112278, https://doi.org/10.1016/j.bios.2020.112278.

[22] J. Su, Y. Ke, N. Maboyi, X. Zhi, S. Yan, F. Li, B. Zhao, X. Jia, S. Song, X. Ding, CRISPR/Cas12a powered DNA framework-supported electrochemical biosensing platform for ultrasensitive nucleic acid analysis, Small Methods 5 (12) (2021), e2100935, https://doi.org/10.1002/smtd.202100935.

[23] J.S. Gootenberg, O.O. Abudayyeh, M.J. Kellner, J. Joung, J.J. Collins, F. Zhang, Multiplexed and portable nucleic acid detection platform with Cas13, Cas12a, and Csm6, Science 360 (6387) (2018) 439–444, https://doi.org/10.1126/science.aaq0179.

[24] S. Lu, X. Tong, Y. Han, K. Zhang, Y. Zhang, Q. Chen, J. Duan, X. Lei, M. Huang, Y. Qiu, D.Y. Zhang, X. Zhou, Y. Zhang, H. Yin, Fast and sensitive detection of SARS-CoV-2 RNA using suboptimal protospacer adjacent motifs for Cas12a, Nat. Biomed. Eng. 6 (3) (2022) 286–297, https://doi.org/10.1038/s41551-022-00861-x.

[25] J. Wang, Q. Xia, J. Wu, Y. Lin, H. Ju, A sensitive electrochemical method for rapid detection of dengue virus by CRISPR/Cas13a-assisted catalytic hairpin assembly, Anal. Chim. Acta 1187 (2021), 339131, https://doi.org/10.1016/j.aca.2021.339131.

[26] L. Liu, Z. Wang, Y. Wang, J. Luan, J.J. Morrissey, R.R. Naik, S. Singamaneni, Plasmonically enhanced CRISPR/Cas13a-Based bioassay for amplification-free detection of cancer-associated RNA, Adv. Healthcare Mater. 10 (20) (2021), e2100956, https://doi.org/10.1002/adhm.202100956.

[27] M. Liang, Z. Li, W. Wang, J. Liu, L. Liu, G. Zhu, L. Karthik, M. Wang, K.F. Wang, Z. Wang, J. Yu, Y. Shuai, J. Yu, L. Zhang, Z. Yang, C. Li, Q. Zhang, T. Shi, L. Zhou, F. Xie, H. Dai, X. Liu, J. Zhang, G. Liu, Y. Zhuo, B. Zhang, C. Liu, S. Li, X. Xia, Y. Tong, Y. Liu, G. Alterovitz, G.Y. Tan, L.X. Zhang, A CRISPR-Cas12a-derived biosensing platform for the highly sensitive detection of diverse small molecules, Nat. Commun. 10 (1) (2019) 3672, https://doi.org/10.1038/s41467-019-11648-1.

[28] M. Rossetti, R. Merlo, N. Bagheri, D. Moscone, A. Valenti, A. Saha, P.R. Arantes, R. Ippodrino, F. Ricci, I. Treglia, E. Delibato, Van der Oost, J, G. Palermo, G. Perugino, A. Porchetta, Enhancement of CRISPR/Cas12a trans-cleavage activity using hairpin DNA reporters, Nucleic Acids Res. 50 (14) (2022) 8377–8391, https://doi.org/10.1093/nar/gkac578.

[29] T. Luo, J. Li, Y. He, H. Liu, Z. Deng, X. Long, Q. Wan, J. Ding, Z. Gong, Y. Yang, S. Zhong, Designing a CRISPR/Cas12a- and Au-Nanobeacon-Based diagnostic biosensor enabling direct, rapid, and sensitive miRNA detection, Anal. Chem. 94 (17) (2022) 6566–6573, https://doi.org/10.1021/acs.analchem.2c00401.

[30] Fei Deng, L. Y, Bitong Li, EwaM. Goldys, Increasing trans-cleavage catalytic efficiency of Cas12a and Cas13a with chemical enhancers: application to amplified nucleic acid detection, Sensor. Actuator. B Chem. 373 (2022), 132767, https://doi.org/10.1016/j.snb.2022.132767.

[31] L.T. Nguyen, B.M. Smith, P.K. Jain, Enhancement of trans-cleavage activity of Cas12a with engineered crRNA enables amplified nucleic acid detection, Nat. Commun. 11 (1) (2020) 4906, https://doi.org/10.1038/s41467-020-18615-1.

[32] M. Zeng, Y. Ke, Z. Zhuang, C. Qin, L.Y. Li, G. Sheng, Z. Li, H. Meng, X. Ding, Harnessing multiplex crRNA in the CRISPR/Cas12a system enables an amplification-free DNA diagnostic platform for ASFV detection, Anal. Chem. 94 (30) (2022) 10805–10812, https://doi.org/10.1021/acs.analchem.2c01588.

[33] D. Zhang, Y. Yan, H. Que, T. Yang, X. Cheng, S. Ding, X. Zhang, W. Cheng, CRISPR/Cas12a-Mediated interfacial cleaving of hairpin DNA reporter for electrochemical nucleic acid sensing, ACS Sens. 5 (2020) 557–562, https://doi.org/10.1021/acssensors.9b02461.

[34] P. Miao, Y. Tang, Gold nanoparticles-based multipedal DNA walker for ratiometric detection of circulating tumor cell, Anal. Chem. 91 (23) (2019) 15187–15192, https://doi.org/10.1021/acs.analchem.9b04000.